The Phantom Burster Model for Pancreatic β-Cells*

Richard Bertram,* Joseph Previte,[†] Arthur Sherman,[‡] Tracie A. Kinard,[§] and Leslie S. Satin[§]
*Institute of Molecular Biophysics, Florida State University, Tallahassee, Florida 32306; [†]School of Science, Pennsylvania State University, Erie, Pennsylvania 16563; [‡]Mathematical Research Branch, National Institute of Diabetes and Digestive and Kidney Diseases, National Institutes of Health, Bethesda, Maryland 20892; and [§]Departments of Pharmacology and Toxicology and Physiology, Medical College of Virginia Campus, Virginia Commonwealth University, Richmond, Virginia 23298-0524 USA

ABSTRACT   Pancreatic β-cells exhibit bursting oscillations with a wide range of periods. Whereas periods in isolated cells are generally either a few seconds or a few minutes, in intact islets of Langerhans they are intermediate (10–60 s). We develop a mathematical model for β-cell electrical activity capable of generating this wide range of bursting oscillations. Unlike previous models, bursting is driven by the interaction of two slow processes, one with a relatively small time constant (1–5 s) and the other with a much larger time constant (1–2 min). Bursting on the intermediate time scale is generated without need for a slow process having an intermediate time constant, hence phantom bursting. The model suggests that isolated cells exhibiting a fast pattern may nonetheless possess slower processes that can be brought out by injecting suitable exogenous currents. Guided by this, we devise an experimental protocol using the dynamic clamp technique that reliably elicits islet-like, medium period oscillations from isolated cells. Finally, we show that strong electrical coupling between a fast burster and a slow burster can produce synchronized medium bursting, suggesting that islets may be composed of cells that are intrinsically either fast or slow, with few or none that are intrinsically medium.

INTRODUCTION

Pancreatic β-cells have been a subject of both experimental and theoretical interest for several decades. One reason for this interest has been the central importance of β-cells for glucose homeostasis. They are the only source of the insulin that most cells require in order to take up and metabolize glucose, and impairment of β-cell function contributes to diabetes. A major focus of theoretical work has been β-cell dynamics, particularly in the form of bursting electrical activity. The bursts consist of active phases of Ca^{2+}-carrying action potentials alternating with silent phases of repolarization and are accompanied by oscillations in cytosolic Ca^{2+}, which drive pulses of insulin secretion (Gilon and Henquin, 1992; Bergsten, 1995; Barbosa et al., 1998).

Electrical activity in β-cells is studied primarily in two distinct preparations: islets of Langerhans, which are micro-organs containing thousands of endocrine cells, and isolated cells. Most work on oscillations has been carried out in the mouse. Bursting has also been recorded *in vivo*, where it can be directly observed to exert negative feedback on plasma glucose levels (Sánchez-Andrés et al., 1995). The only stimulus required for oscillations *in vitro* is elevation of glucose to levels between 5 and 20 mM, which results in bursts ranging from 10 to 60 s. Faster oscillations, of 10 s or less, are induced by acetylcholine, a physiological potentiator of glucose-dependent insulin secretion (Bertram et al., 1995). Slower oscillations, with periods of several minutes, are induced by epinephrine, a physiological inhibitor of

insulin secretion (Cook and Perara, 1982). Slower oscillations in membrane potential and/or Ca^{2+} have also been reported in the presence of leucine or ketoisocaproate (Martin et al., 1995; Martin and Soria, 1995) and high external Ca^{2+} (Gilon and Henquin, 1992), and there is evidence that culturing islets for several days favors the appearance of slow oscillations (Gilon et al., 1994; Bergsten, 1995; Liu et al., 1998; but see Roe et al., 1995).

Single-cell electrophysiological studies (Kinard et al., 1999; Falke et al., 1989) have established that single cells can burst as well as spike repetitively, but this bursting is typically much faster than that in islets (period 2–5 s; see Fig. 1 *A*). Sometimes bursts much slower than those in islets (period 1–6 min) are seen (Larsson et al., 1996; Smith et al., 1990; Fig. 1 *C* this paper). Slow oscillations, presumably reflecting slow bursting electrical activity, predominate in Ca^{2+} imaging studies of isolated cells and small cell clusters (Larsson et al., 1996; Leech et al., 1994; Liu et al., 1994, 1995; Miura et al., 1997). Bursting with a period comparable to that in islets is seen (Fig. 1 *B*), but only rarely.

It is not clear whether the fast and slow bursting modes seen in islets operate by the same mechanisms as the corresponding oscillatory modes in dispersed cells. However, this diversity of behavior does not seem to be artifactual, but rather to reflect a diversity of mechanisms present in both single cells and islets to varying degrees in various circumstances. Our goals, then, are twofold: To develop a model for β-cell bursting that can account in a natural way for oscillations on time scales covering two orders of magnitude, and to explain why islets predominantly exhibit the medium mode and single cells predominantly exhibit the fast and slow modes.

All models to date have essentially relied on negative feedback from a single slow process, retaining the basic
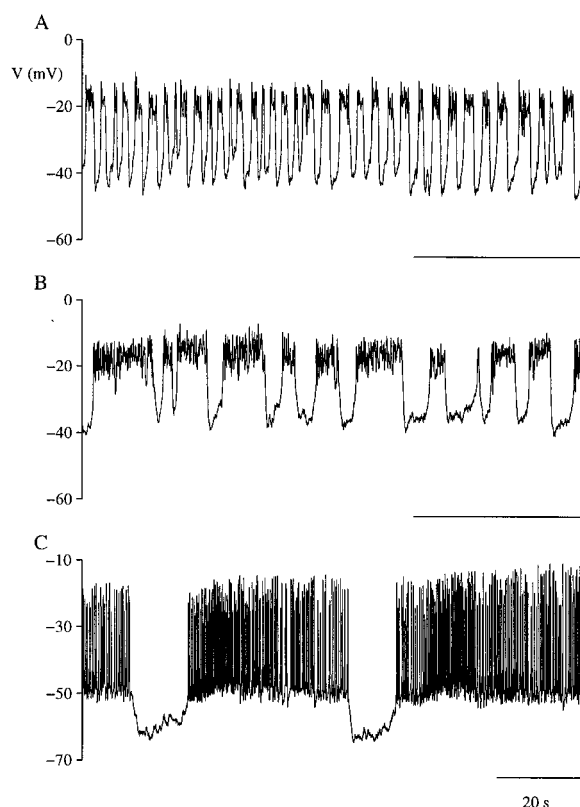

FIGURE 1 Burst patterns on fast (*A*), medium (*B*), and slow (*C*) time scales. Of 50 cells observed, 24 were fast, 3 were medium, and 1 was slow. The remainder were non-bursters, 19 spikers and 3 plateau cells. Traces were recorded using current clamp and the perforated patch technique from single cells (*A, B*) and a small cluster (*C*). The time bar represents 20 s for all traces.

structure of the first model (Chay and Keizer, 1983). Following a proposal of Atwater et al. (1980), Chay and Keizer incorporated negative feedback by a slow accumulation of cytosolic Ca^{2+}, acting on a Ca^{2+}-activated K^+ (K(Ca)) channel. Successor models have differed primarily in the candidate negative-feedback processes considered. These have included inactivation of a Ca^{2+} current (Chay and Cook, 1988; Keizer and Smolen, 1991), cytosolic ATP/ADP acting on a K(ATP) channel (Keizer and Magnus, 1989; Smolen and Keizer, 1992; Magnus and Keizer, 1998), or the Ca^{2+} concentration in the endoplasmic reticulum (ER) (Ca_{er}). The latter has been proposed both to act on calcium release-activated channels (CRAC; Roe et al., 1998; Chay, 1996) and to modulate the effect of Ca^{2+} on Ca^{2+} or K^+ channels (Chay, 1997; Gall and Susa, 1999).

These models have mostly addressed islet bursting on the medium time scale, the scale for which there is the least evidence for a candidate slow process. Indeed, 20 years of searching have characterized several processes that vary on time scales of less than 10 s (K(Ca), Ca^{2+} channel inactivation) and suggested several candidates that may vary on time scales of more than 1 min (K(ATP), Ca_{er}), but nothing

has been shown convincingly to vary on a time scale of tens of seconds.

This leads us to propose a model in which medium bursting results from the synergistic interaction between two variables, one with a time constant of 1 to 5 s, the other with a time constant of 1 to 2 min. Thus, both are slow in comparison to the fast spiking variables, which vary on a time scale of tens of milliseconds, but one is much slower than the other. In one parameter regime, the faster of the two slow processes dominates and drives fast bursting. In another regime, the slower process dominates, and slow bursting is produced. In yet a third regime, the two slow processes interact to produce medium bursting, although neither process alone has a time constant appropriate for this mode of bursting. Thus, there need not be a distinct entity operating on the time scale of medium bursting, but rather a composite of faster and slower processes, which we call "phantom bursting." We further suggest that in islets, electrical coupling of fast and slow cells leads to a collective medium rhythm, which cannot easily be obtained in isolation.

A further implication of the phantom model is that isolated cells exhibiting fast oscillations also possess a slow pacemaker process, which is not manifest because it is masked by a faster process. Simulations with the model suggest that slower oscillations could be induced by injecting a current with suitable kinetics to partially nullify the faster process, allowing the slower process to emerge. Using the dynamic clamp technique (Kinard et al., 1999), we are indeed able to elicit medium period bursts from isolated cells that previously exhibited only fast bursting or spiking (see Fig. 9).

For concreteness, we describe below a particular biophysical realization of the phantom model, showing its capability to produce multiple modes of bursting. However, we stress that the phantom idea is quite general and can work with a wide range of possible identities for the two slow inhibitory variables. To emphasize this, we also present the phantom phenomenon using a geometrical phase-plane analysis, illustrating how other channel mechanisms could work equally well within the phantom framework, and generalizing the classical analysis of the Chay-Keizer family of models (Rinzel and Ermentrout, 1998). Finally, with the assistance of the model, we design and carry out experiments in which dynamic-clamp is used to convert fast oscillations to medium bursts. In addition to confirming a key element of the model, we thus demonstrate for the first time a reliable experimental protocol for eliciting islet-like bursts from isolated β-cells.

METHODS

Cell culture

Pancreases were isolated from Swiss-Webster mice by collagenase digestion to yield single islets (Hopkins et al., 1991; Kinard and Satin, 1996).

Islets were then dispersed into single cells by gently shaking them in a low calcium medium. Cells were cultured in RPMI-1640 with fetal bovine serum, L-glutamine, and penicillin/streptomycin. Cells were seeded onto glass cover slips placed in 35-mm petri plates and kept at 37°C in an air/CO$_2$ incubator. Except where noted, studies focused on isolated single cells, which were selected by appearance.

Electrophysiology and solutions

Mouse β-cells were placed in a recording chamber on the stage of an inverted microscope (Olympus IX50, Tokyo, Japan). The chamber was continuously superfused with an external solution that contained, in mM, 115 NaCl, 3 CaCl$_2$, 5 KCl, 2 MgCl$_2$, 10 HEPES, and 11.1 glucose, pH 7.2. Experiments were performed using perforated patch clamp. Pipette tips were filled with a solution containing, in mM, 28.4 K$_2$SO$_4$, 63.7 KCl, 11.8 NaCl, 1 MgCl$_2$, 20.8 HEPES, and 0.5 EGTA, pH 7.2. Pipettes were pulled on a two-stage horizontal puller (Sutter Instruments, Novato, CA) and had resistances ranging from 4 to 10 MΩ. The pipettes were then back-filled with the same internal solution containing 0.1 mg/ml amphotericin-B (Rae et al., 1991). Each electrode was then placed on a cell and a gigaohmic seal was obtained. It usually took 5 to 15 min to obtain adequate steady-state patch perforation, and experiments did not commence until a steady zero current potential was obtained. Experiments were performed at 35°C. The recording chamber was heated using a TC-1 temperature controller and H-1 heater (Cell Micro Controls, Virginia Beach, VA). Bath temperature was measured at the bottom surface of the recording chamber with a TH-1 thermocouple probe. An Axopatch 200B patch clamp amplifier (Axon Instruments, Foster City, CA) was used in the standard tight-seal perforated patch-clamp mode to analyze membrane potential under current-clamp conditions (Hamill et al., 1981). Seal resistances obtained were >5 GΩ.

Dynamic clamping

Dynamic clamp (Sharp et al., 1993; Ma and Koester, 1996; Turrigiano et al., 1996; Kinard et al., 1999) differs from standard current clamp in that the current injected is based on the calculated response of a hypothetical voltage-dependent conductance to cell membrane potential at each instant in time. To implement dynamic clamp, membrane potential was rapidly sampled via a 12-bit A/D-D/A board (Digidata 1200, Axon Instruments) in current clamp and scaled appropriately. Artificial currents based on the measured membrane potential were calculated in software (Dclamp, Dyna-Quest Technologies, Sudbury, MA) running on a PC (Micron Electronics, Nampa, ID) and scaled appropriately. Driving voltages were sent out from the D/A converter and filtered at 10 kHz while cell membrane potentials were acquired at 20 kHz, using a VCR recorder (DR 8900, Neurodata Corp., New York, NY) for off-line analysis. For playback, taped voltage data was digitized at 200 Hz after low pass filtering at 100 Hz. Because the computer running D-clamp cannot simultaneously be used for data acquisition, this was done with a Power Macintosh G3 computer (Apple Computer, Cupertino, CA), a 16-bit, 200 kHz hardware interface (IPC16, Instrutech, Elmont, NY 11003), IgorPro 3.0 software (Wavemetrics, Lake Oswego, OR) and Pulse Control software (Herrington and Bookman, 1994).

Dynamic clamp was used here as a way to nullify, at least partially, a current whose identity and pharmacology were unknown, but which was hypothesized on the basis of the model described below to be either a slowly activating outward current or a slowly inactivating inward current. Thus, an artificial inward current (reversal potential, 100 mV) with slow activation (rate $\sim$0.2–20.0 s^{-1}) was calculated according to Eqs. 12–14 and injected. See "Experimental test of the model" section of Results, below, for details.

Some aspects of these investigations have appeared in abstract form (Bertram et al., 2000).

Modeling

Like previous β-cell models, the phantom model consists of a subset of fast variables (fast subsystem) that govern spiking during the active phase of a burst, and slow negative feedback to switch the spiking on and off. The fast subsystem consists of two equations, the minimum number, for membrane potential, V, and the fast K$^+$ current activation variable n. The new element of the model is the essential participation of two distinct slow negative feedback variables, which we will denote simply as s_1 and s_2. One previous β-cell model included two slow negative feedback variables (Keizer and Smolen, 1991), and could produce a variety of bursting patterns (Smolen et al., 1993b). However, β-cell-like bursting was due to the slow oscillation of a single variable in this model. In comparison with previous models, s_1, with a time constant of 1 s, is only marginally slower than the fast variables, which operate on a time scale of tens of milliseconds. In contrast, s_2 is very slow, having a time constant of 120 s. In the simulations that follow, s_1 drives the fast oscillations, with period <10 seconds; s_2 drives the slow oscillations, with period >60 s; and the interaction of s_1 and s_2 drives the medium oscillations with period between 10 and 60 s. We have chosen for illustration an extreme discrepancy between the time constants of s_1 and s_2; the time constant of s_1 could be made as large as 10 s, and that of s_2 as small as 1 min. The equations are:

$$\frac{dV}{dt} = -(I_{Ca} + I_K + I_{s1} + I_{s2} + I_L)/C_m \quad (1)$$

$$\frac{dn}{dt} = (n_\infty(V) - n)/\tau_n \quad (2)$$

$$\frac{ds_1}{dt} = (s_{1\infty}(V) - s_1)/\tau_{s1} \quad (3)$$

$$\frac{ds_2}{dt} = (s_{2\infty}(V) - s_2)/\tau_{s2} \quad (4)$$

The ionic currents are:

$$I_{Ca} = g_{Ca}m_\infty(V)(V - V_{Ca}), \quad I_K = g_K n(V - V_K) \quad (5)$$

$$I_{S1} = g_{s1}s_1(V - V_K), \quad I_{S2} = g_{s2}s_2(V - V_K) \quad (6)$$

$$I_L = g_L(V - V_L). \quad (7)$$

I_{Ca} is a Ca^{2+} current that activates instantaneously, I_K is a rapidly activating K$^+$ current, and I_L is a leak current.

Although the slow currents, I_{s1} and I_{s2}, are formulated here as K$^+$ currents for concreteness, their biophysical identities remain obscure. However, as an illustrative example, one may think of I_{s1} as a K(Ca) current, activated by cytosolic Ca^{2+}, and of I_{s2} as a K(ATP) current, activated by an increase in [ADP] relative to [ATP]. Neither of these currents is voltage-dependent, but K(Ca) responds to the rise in cytosolic [Ca^{2+}]$_i$ that follows depolarization, and it has been suggested that K(ATP) current might also increase with [Ca^{2+}]$_i$ as a result of either hindered ATP production (Keizer and Magnus, 1989; Magnus and Keizer, 1998) or enhanced ATP consumption (Detimary et al., 1998). For our purposes it is sufficient that I_{s1} and I_{s2} are repolarizing, negative feedback currents that turn on when the cell is depolarized. Indeed, the model works equally well if either or both are depolarizing inward currents that turn off or inactivate when the cell is depolarized. There are a number of parameters that could be varied to produce a wide range of burst periods; below, we will vary the maximal conductance, g_{s1}, of I_{s1}.

The activation curves for m, n, s_1, and s_2 are sigmoidal Boltzmann functions, increasing with membrane potential:

$$m_\infty(V) = \frac{1}{1 + \exp[(-22 - V)/7.5]}, \tag{8}$$

$$n_\infty(V) = \frac{1}{1 + \exp[(-9 - V)/10]}$$

$$s_{1\infty}(V) = \frac{1}{1 + \exp[(-40 - V)/0.5]}, \tag{9}$$

$$s_{2\infty}(V) = \frac{1}{1 + \exp[(-42 - V)/0.4]}$$

The only voltage-dependent time constant is that for the K$^+$ conductance activation variable, n:

$$\tau_n(V) = \frac{8.3}{1 + \exp[(V + 9)/10]}. \tag{10}$$

The other time constants and parameter values are listed in Table 1 and the figure legends. Expressions and parameters for the fast ionic currents, equilibrium and time constant functions, and parameter values are adapted from an earlier β-cell model (Chay and Cook, 1988). The inhibitory role of the slow, voltage-dependent inactivation of I_{Ca} was replaced by the effects of s_1, and the fast Ca^{2+}-dependent inactivation was omitted for the sake of simplicity. Consequently, the Ca^{2+} current is about an order of magnitude smaller than experimentally measured values (see, e.g., Göpel et al., 1999a). As a result, the slow currents, I_{s1} and I_{s2}, may be expected to understate to a similar degree those in real cells. Other obvious omissions from the model are cytosolic and ER Ca^{2+}. The possible contributions of these two key calcium pools to s_1 and s_2 are treated in passing below and in detail in the Discussion.

RESULTS

Fast bursting

Fast bursting is obtained by setting g_{s1} to a relatively large value of 20 pS. Numerical integration of Eqs. 1–4 then yields the results shown in Fig. 2. The bursts are driven by a slow activity-dependent oscillation in s_1 (Fig. 2 B). When s_1 is small, the hyperpolarizing current I_{s1} is too weak to hold the membrane potential below the spike threshold, so action potentials are produced. This spiking activity in turn
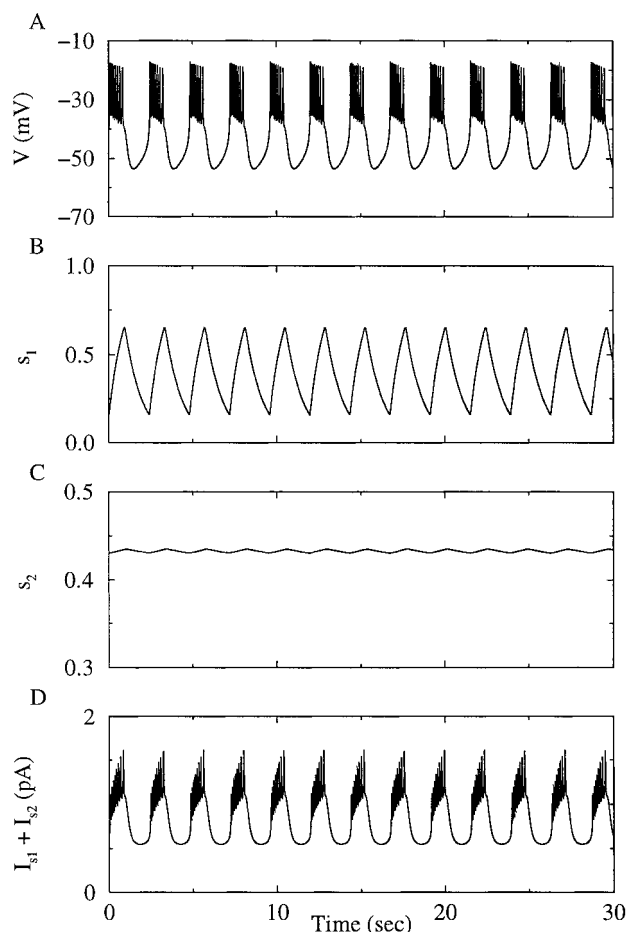

FIGURE 2 Fast bursting generated with g_{s1} = 20 pS. The bursting, with a period of 3 s, is driven by activity-dependent oscillations in the K$^+$ activation variable s_1. Although oscillations in the slow variable s_2 are unimportant, the mean value of s_2 affects the bursting by determining the average level of the hyperpolarizing I_{s2} current.

causes s_1 to slowly increase, activating I_{s1}. When s_1 is sufficiently large, I_{s1} suppresses the action potentials, and the cell returns to a hyperpolarized silent state. In other words, the bursts are driven by the negative feedback of s_1 as in Chay-Keizer and all subsequent β-cell models, but the period is limited to 3 s by the small (1 s) time constant of s_1.

Note that s_2 remains essentially constant. This is because the dynamics of s_2 are too slow (i.e., 2 min) to allow for significant variation during a burst, so s_2 simply oscillates with a small amplitude about its mean value of about 0.43 (Fig. 2 C). However, if the mean value were increased by a leftward shift in the $s_{2\infty}$ function, the mean hyperpolarizing I_{s2} current would increase and shorten the active phase of bursting. Thus, in the case of fast bursting, oscillations in s_2 are unimportant, but the mean value of s_2 does regulate bursting by setting the mean activation of the hyperpolarizing current I_{s2}. Fig. 2 D shows the total slow current, I_{s1} + I_{s2}. It is this net current that determines the cycling between active and silent phases, not the individual components.

TABLE 1 Default parameter values

Symbol	Description	Value
C_m	membrane capacitance	4524 fF
g_{Ca}	fast Ca^{2+} current conductance	280 pS
g_K	fast K$^+$ current conductance	1300 pS
g_L	leakage current conductance	25 pS
g_{s1}	slow K$^+$ conductance	3–20 pS
g_{s2}	very slow K$^+$ conductance	32 pS
V_{Ca}	Ca^{2+} reversal potential	100 mV
V_K	K$^+$ reversal potential	−80 mV
V_L	leakage reversal potential	−40 mV
τ_{s1}	s_1 time constant	1 s
τ_{s2}	s_2 time constant	2 min

Another feature of the fast bursting is the relatively depolarized silent phase (compare Figs. 2 and 3). This is a consequence of s_1 being only marginally slow compared to the fast variables, which does not allow V time to repolarize completely during the silent phase before the next active phase begins. This depolarized silent phase is a typical feature of the fast bursting recorded in single β-cells (Fig. 1 A and Kinard et al., 1999; Falke et al., 1989). It is also seen in the fast bursting of islets exposed to acetylcholine or other muscarinic agonists (Bertram et al., 1995). This does not mean that the mechanisms of fast bursting in single cells and islets are necessarily the same, but it suggests that the slow variables driving bursting in both cases may similarly be marginally slow.

Medium bursting

If the maximal s_1 conductance, g_{s1}, is reduced, the burst period will increase. This is because s_1 will have to increase further to produce the same level of inhibition during the active phase, and will have to decrease further during the
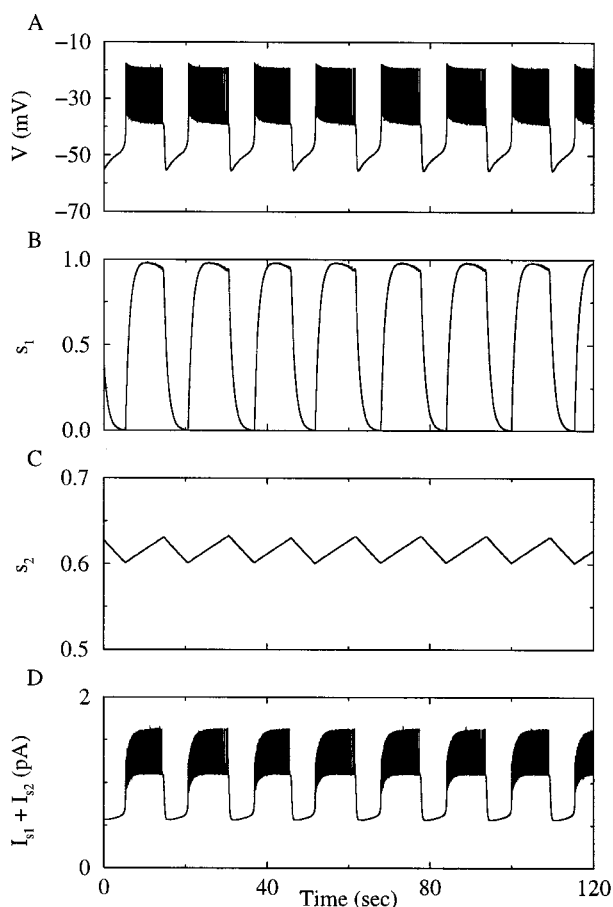

A

B

C

D

FIGURE 3   Medium phantom bursting produced with $g_{s1} = 7$ pS. The bursts, with a period of 15 s, are generated by activity-dependent oscillations in both s_1 and s_2. Note the change in time scale from Fig. 2.

silent phase recovery. Thus the period depends not only on the time constant of s_1, but also on the extent to which s_1 must change in order to exert its effect. In principle, one could in this manner make the period arbitrarily long, but in practice one finds that if g_{s1} is reduced too much, even maximal activation of s_1 is unable to terminate an active phase. Then, s_1 stalls at its maximum value of 1, and the cell spikes continuously. In the phantom model, however, there is a second slow variable, s_2, which has an opportunity to increase when s_1 hangs up. When s_2 has increased sufficiently, the burst is able to terminate. This is illustrated in Fig. 3 where g_{s1} has been reduced from 20 to 7 pS. For this value of g_{s1}, only a small increase in s_2 is required to supplement the negative feedback from s_1, and the active phase duration is intermediate between that observed with s_1 or s_2 alone. In the ensuing silent phase, the decrease of s_1 to 0 is insufficient to reinitiate spiking, because the accumulated s_2 from the active phase also needs time to recover. Therefore the duration of the silent phase is also intermediate between that when s_1 or s_2 alone mediates the repolarization. The oscillations in s_2 are now significantly larger than in the fast bursting case, when s_1 was solely responsible for initiating and terminating the bursts. Though still modest, they are nonetheless mandatory, for without them the cell would spike continuously. The oscillations in s_1 are also necessary; without them, the burst period would be governed by the time scale of s_2 alone, and would last minutes rather than tens of seconds. Note that the active and silent phases end at the same levels of total slow current as in Fig. 2 D.

Slow bursting

Further reduction in g_{s1} leads to a further increase in burst period because the less g_{s1} available, the more s_2 has to vary to compensate (we assume that g_{s2} is fixed). Furthermore, as these changes in s_2 are very slow, the burst period increases rather steeply as g_{s1} is reduced below 7 pS. Fig. 4 illustrates full-blown slow bursting with a period of more than 1.5 min for $g_{s1} = 3$ pS. Now s_1 spends almost all the time stalled at its maximum or minimum values, and s_2 must change substantially because it carries nearly the full burden of burst pacing. In Fig. 5 we show the dependence of burst period on g_{s1}. Note that only a relatively small range of g_{s1} values gives medium bursting, which may shed light on why this behavior is not often seen in isolated cells.

If we pursue the interpretation of g_{s2} as a K(ATP) conductance, then Figs. 2, 3, and 4 suggest that oscillations in K(ATP) conductance are small and possibly undetectable during fast and medium bursting, but large and potentially detectable during slow bursting. We note that variations in K(ATP) conductance between silent and active phases have been observed only in slow bursting (Larsson et al., 1996), though not universally even in that case (Smith et al., 1990).
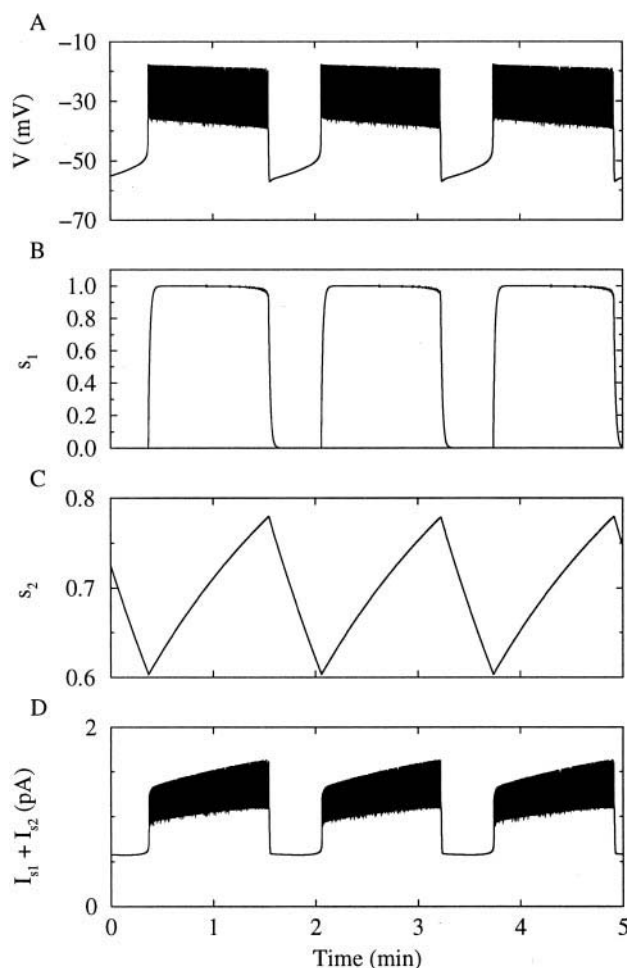
FIGURE 4 Slow bursting produced with $g_{s1} = 3$ pS. The bursts, with a period of more than 1.5 min, are generated by slow activity-dependent oscillations in s_2 alone, whereas s_1 exhibits a square-wave oscillation.

Phase-plane analysis

Additional insight can be gained by analyzing the model geometrically in phase space, that is, by examining the trajectories of the dependent variables with time omitted (Figs. 6 and 7). This analysis also makes clear that any model with certain geometrical features could exhibit the
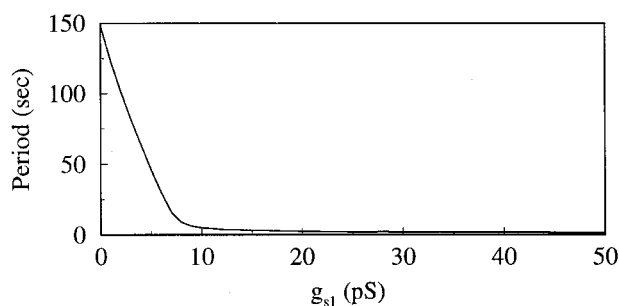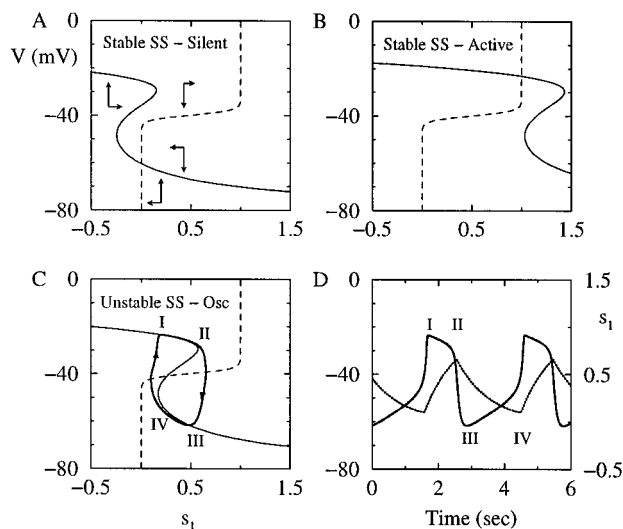

FIGURE 5 Dependence of burst period on g_{s1}.

FIGURE 6 Phase plane analysis of fast bursting. The system is reduced to two variables by setting $n = n_\infty(V)$ and fixing s_2 at 1.0 (A), −1.0 (B), and 0.346 (C and D). Parameters are as in Fig. 2 except the slope factor for the Boltzmann function $s_{1\infty}(V)$ in Eq. 9 is 1, and $g_{s1} = 50$ pS. In A–C, *light solid curves* are V nullclines, *dashed curves* are s_1 nullclines. *Heavy solid curve* is the V-s_1 trajectory in C and V time course in D. *Dotted line* in D is the s_1 time course. SS, steady state. See text for details.

phantom phenomenon, which is not limited to models having the particular ion channels employed in the example discussed in this paper. For a general tutorial on the application of phase-plane methods to Hodgkin-Huxley type models and bursting, see Rinzel and Ermentrout (1998).

The analysis can be simplified without losing any essential features for our purposes by reducing the system to two dimensions and thus reducing the 3D phase space to a 2D phase plane. This requires two small changes in the equations. First, we set the delayed-rectifier gating variable n to equal its steady-state activation function, $n = n_\infty(V)$ in Eq. 5. This eliminates spiking, leaving only plateaus, which can be thought of roughly as representing the average membrane potential during a burst. Second, to analyze fast bursting (Fig. 6) we can hold s_2 constant because s_2 is nearly constant in that case anyway (see Fig. 2 C). For medium and slow bursting, s_2 can no longer be considered constant (Figs. 3 C and 4 C), but it varies slowly enough that the other variables can be considered to be in a quasi-steady state. The graphical description of medium and slow bursting then requires a series of slowly varying phase-plane snapshots (Fig. 7).

The trajectories in the phase plane can be predicted qualitatively by considering the regions of the plane in which each of the variables V and s_1 increases and decreases. The regions are separated by balance curves (nullclines) along which the derivatives of V and s_1 are zero. The solid Z-shaped curves in Fig. 6, A–C indicate where $dV/dt = 0$, and are obtained by setting the right-hand side of
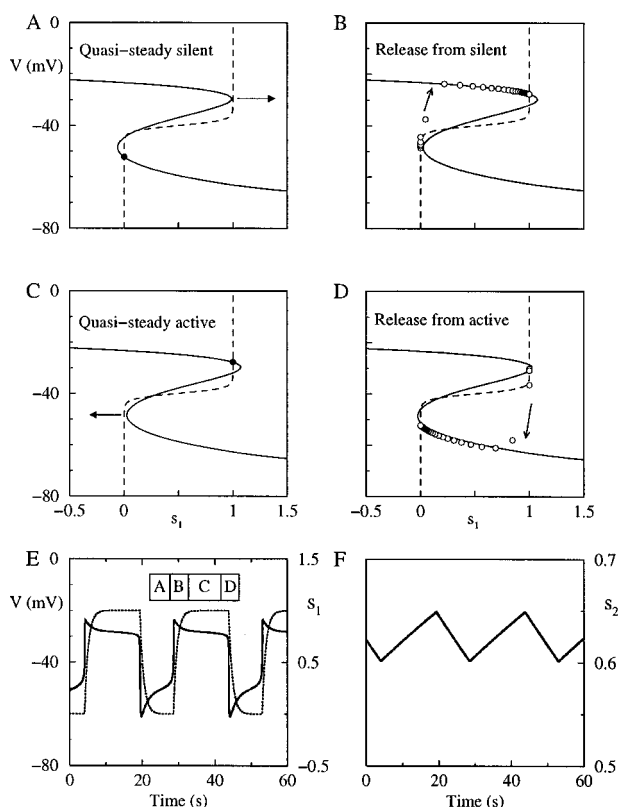
FIGURE 7 Phase plane analysis of phantom medium bursting. Parameters are as in Fig. 6, except that g_{s1} is reduced to 19 pS, and s_2 is now allowed to vary. (A–D) V-s_1 phase planes. *Light solid Z-shaped curves are* V nullclines; *dashed curves are* s_1 nullclines. *Horizontal arrows in* A *and* C indicate slow motion of Z-curves. *Oblique arrows in* B *and* D indicate motion of V-s_1 phase point. The *empty circles in* B *and* D are equally spaced in time so larger gaps indicate faster motion. (E–F) V, s_1, and s_2 time courses corresponding to phase planes. Bars labeled A–D in E indicate time intervals corresponding to those panels. *Heavy solid curve in* E *is* V; *dotted curve is* s_1. See text for details.

Eq. 1 to zero. Although Eq. 1 cannot be solved for V, it can easily be solved for s_1:

$$s_1 = -\frac{I_{Ca}(V) + I_K(V) + I_L(V)}{g_{s1}(V - V_K)} - \frac{g_{s2}}{g_{s1}} s_2 \qquad (11)$$

The vertical arrows in Fig. 6 A indicate that V increases to the left of the Z-curve and decreases to the right. Similarly, the dashed, sigmoidal curves in Fig. 6, A–C are defined by $ds_1/dt = 0$ and satisfy the simple equation $s_1 = s_{1\infty}(V)$; see Eq. 3. The horizontal arrows in Fig. 6 A indicate that s_1 increases to the left of the sigmoid and decreases to the right. The lengths of the arrows, though not to scale, indicate that s_1 changes more slowly than V. Where the Z-curve and sigmoid intersect, the derivatives of both V and s_1 are 0, and the system is at a steady state. That is, if the trajectory lands on this intersection, it will remain there because neither V nor s_1 can change. Further, the arrows in Fig. 6 A tell us that this steady state is stable: If the trajectory is

perturbed away from the point of intersection, it will return. In fact, given any initial values for V and s_1, the system will end up in this low-voltage steady state.

If s_2 is decreased, the Z-curve shifts to the right; the loss of negative feedback from s_2 must be made up by an increase in s_1. This can also be seen from Eq. 11, which shows that for each value of V, s_1 becomes larger. For sufficiently small s_2, the s_1 nullcline intersects the upper branch of the V nullcline (Fig. 6 B), and the system will always end up in a high-voltage steady state. (If n is not set equal to $n_\infty(V)$, this active state will be oscillatory, i.e., the cell will spike continuously.) The most interesting case occurs for intermediate values of s_2, for which the steady state lies on the middle branch of the Z-curve (Fig. 6 C). Such steady states are unstable, having the character of threshold points, because V will increase if perturbed upward and decrease if V is perturbed downward. Full explication of this case is more subtle, but it is plausible from the regions of increase and decrease for V and s_1 that the system will oscillate, passing through an endless cycle of active and silent states. This is rigorously true if s_1 is sufficiently slow compared to V (Rinzel and Ermentrout, 1998). The behavior of V (solid) and s_1 (dotted) in the time domain is plotted in Fig. 6 D, with the Roman numerals I–IV indicating the correspondence between time points and points on the trajectory in the V-s_1 plane.

Every β-cell model published to date can essentially be reduced to Fig. 6. The only difference between fast bursting in the phantom model and the (medium) bursting in prior models is the magnitude of the time constant of s_1. Here the burst period is short (about 3 s) because the time constant of s_1 is small (1 s). Increasing τ_{s1} does not change the configuration of nullclines in Fig. 6, but it slows the cycling through the points I–IV. An alternative way to increase burst period is to stretch the V nullcline by reducing g_{s1}. Eq. 11 shows that reducing g_{s1} by, say, a factor of two stretches every point on the V nullcline to the right by a factor of two. Like decreasing s_2, this shifts the Z-curve to the right, but it also increases the distance between the left and right knees proportionally.

There is a limit to how much the period can be increased by such stretching. Bursting that depends on variation only in s_1, not s_2, requires that the s_1 and V nullclines intersect exactly once on the middle branch of the V nullcline as in Fig. 6 C, and if the Z-curve is stretched too far, this cannot occur. There will always be a stable steady state on either the lower branch of the Z-curve (for larger values of s_2, as in Fig. 7 A), or the upper branch (for smaller values of s_2, as in Fig. 7 C), or both. On the other hand, if s_2 is not fixed, but rather follows the dynamics of Eq. 4, medium bursting results as described above in the section on medium bursting. The sequence of phase planes in Fig. 7, A–D, illustrates this from the geometrical perspective.

Starting with a high value of s_2, the system is in the configuration of Fig. 7 A. The membrane potential is low,

which causes s_2 to decrease (Eqs. 4 and 9), pulling the Z-curve to the right (Eq. 11). Thus, the intersection of the nullclines is a quasi-steady state, with membrane potential slowly ramping up. When the intersection reaches the left knee of the Z-curve, the phase point is released and flows up to the upper branch of the Z-curve (Fig. 7 B). However, a new intersection appears on the upper branch, leading to a quasi-steady state with elevated membrane potential (Fig. 7 C). This causes s_2 to increase, pulling the Z-curve slowly to the left. When the phase point reaches the right knee of the Z-curve, it is released and flows down to the lower branch (Fig. 7 D). The four phase planes correspond to intervals A–D in the time domain (Fig. 7 E). One complete cycle includes two intervals (B and D) in which s_1 makes rapid transitions and two intervals in which s_1 stalls (A and C).

Figure 7 represents a case where g_{s1} is just below the critical value at which stalling first occurs, and so the variation in s_2 is small (Fig. 7 F). However, s_2 is so much slower than s_1 that its contribution to the period is greater, and the period is already much longer than that with s_1 alone. Further decreases in g_{s1} stretch the Z-curve further, so that it extends further beyond the extremes of the s_1 nullcline. Then more time is spent in the quasi-steady intervals relative to the fast transitions, and the burst period and the variation in s_2 increase until the fully developed slow regime is reached.

Together, Figs. 6 and 7 illustrate that the fundamental requirements for phantom bursting are (i) two slow variables with time constants smaller and larger, respectively, than the time scale of medium bursting, and (ii) a parameter that deforms the s_1 or s_2 nullclines in such a way that multiple stable intersections occur, so that s_1 can not preempt s_2. In the particular instance of phantom bursting described here, we accomplished this by reducing g_{s1} and thereby stretching the Z-curve. Two other ways are to vary the sharpness of the s_1 nullcline or to shift the s_1 nullcline upward (for a graded range of periods in the latter case, the nullcline should not be too sharp). These changes also prevent the two nullclines from intersecting only on the middle branch of the Z-curve, causing s_1 to stall and allowing s_2 to go into motion. The approach outlined here is, then, a template for constructing a family of models, which differ in possibly important details, but which all display multiple modes of bursting.

Experimental test of the model

A thorough test of the phantom hypothesis and its many possible realizations would require detailed knowledge of all the ionic currents in β-cells, which is beyond the scope of this study. Here we present a limited set of experiments that test an important prediction of the model, lending support to its central hypothesis. We ask whether isolated cells, which typically exhibit fast rhythms rather than the

medium rhythms of islets, in fact possess a slow process (or processes) that is pre-empted by a faster one.

In our hands, isolated cells predominantly exhibit fast bursting with a period of <5 s or large-amplitude continuous spiking (Kinard et al., 1999). Occasionally, however, we see medium (Fig. 1 B) or slow (Fig. 1 C) bursting, the latter generally in small cell clusters. The model predicts that fast bursters can be converted to medium or slow bursters by reducing the maximal conductance g_{s1} of a negative feedback current having a time constant of at most a few seconds. As we do not know the explicit identity of g_{s1}, and for some candidate channels there are no pharmacological blockers available, we use dynamic clamp to partially nullify it. This can be done by adding to single β-cells an inward current that develops over the time scale of a few seconds. Alternatively, one can subtract an outward current with similar kinetics. We illustrate the former here, but have successfully used both types of currents to modify fast bursting.

The artificial dynamic clamp current was formulated using the simple V-rate-independent form available in the D-clamp software. It activated slowly with a rate independent of membrane potential, had a Boltzmann type voltage-dependent activation curve, and lacked inactivation:

$$I_{Clamp} = G_{max}z(V - V_r) \qquad (12)$$

where z satisfies the differential equation

$$\frac{dz}{dt} = K(z_\infty(V) - z), \qquad (13)$$

and

$$z_\infty(V) = \frac{1}{1 + \exp[(-22 - V)/7.5]}. \qquad (14)$$

Note that this current, unlike a DC applied current, will do nothing in an electrically silent, hyperpolarized cell; the cell must first depolarize sufficiently for z to respond. We will see, however, that I_{Clamp} has dramatic effects on the behavior of cells that are oscillatory, and hence depolarize spontaneously. With $V_r = 100$ mV, I_{Clamp} resembles the Ca^{2+} current in the model (see Eq. 5), but has a fixed (non-V-dependent) time constant rather than instantaneous activation. The precise form of the current matters less than its kinetics and polarity. Artificial outward current was subtracted by making G_{max} negative and setting V_r to −90 mV.

Note that we are not suggesting that a Ca^{2+} current with the properties of I_{Clamp} exists in β-cells; this is merely an experimental maneuver that the model predicts would be effective in cancelling out the faster slow process corresponding to s_1 that masks the presence of s_2.

We first tested the protocol by simulating it with the model. Figure 8 illustrates conversion of a model fast burster (same parameters as in Fig. 2) to a medium burster following addition of I_{Clamp} with $G_{max} = 0.015$ nS and $K =$
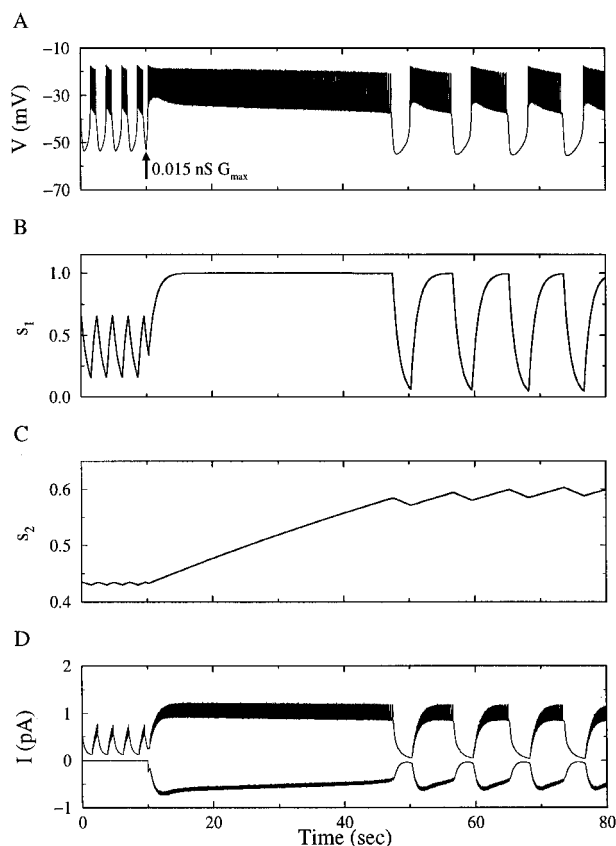
FIGURE 8 Simulated dynamic clamp protocol. Artificial inward current (Eqs. 12–14) with $G_{max} = 0.015$ nS and $K = 2.0$ s^{-1} added to model equations at $t = 10$ s. In D, I_{s1} is the current with upward deflections and I_{Clamp} the current with downward deflections.

FIGURE 9 Experimental conversion of fast single β-cells to medium bursting using dynamic clamp. (A) A fast bursting cell converted to medium bursting by injection of artificial clamp current (Eqs. 12–14) with G_{max} as indicated and $K = 2.0$ s^{-1}. (B) Same for fast spiking cell. (C) The artificial clamp current used in B. Representative of 20 successful conversions out of 31 cells attempted, using G_{max} in the range 0.002–0.030 nS.

2.0 s^{-1} (time constant 500 ms). After a transient, medium bursting with a period of about 10 s is seen (Fig. 8 A), accompanied by s_2 oscillations having substantially larger amplitude (Fig. 8 B). The exogenous current required for the conversion to occur is rather small, less than 1 pA (Fig. 8 C). The current develops as an approximate mirror image of I_{s1}, preventing s_1 from repolarizing the cell and allowing oscillations in s_2 to emerge.

Guided by the model, we applied the procedure to β-cells. Fig. 9, A and B, shows successful conversions of two different single cells to markedly slower rhythms. Cell A was initially a fast burster, whereas cell B is of particular note because it was initially a fast spiker, with no hint of plateau behavior before the addition of I_{Clamp}. In both cases, the cells reverted to their original fast pattern once the exogenous current was removed. In some other cells tested, cell firing patterns remained altered after termination of the stimulus, but in all cases the period decreased markedly towards the control value. Of 20 cells where the addition of depolarizing current with dynamic clamp produced more prolonged bursting, 16 displayed patterns resembling the medium bursting of islets. For 11 other cells, the addition of
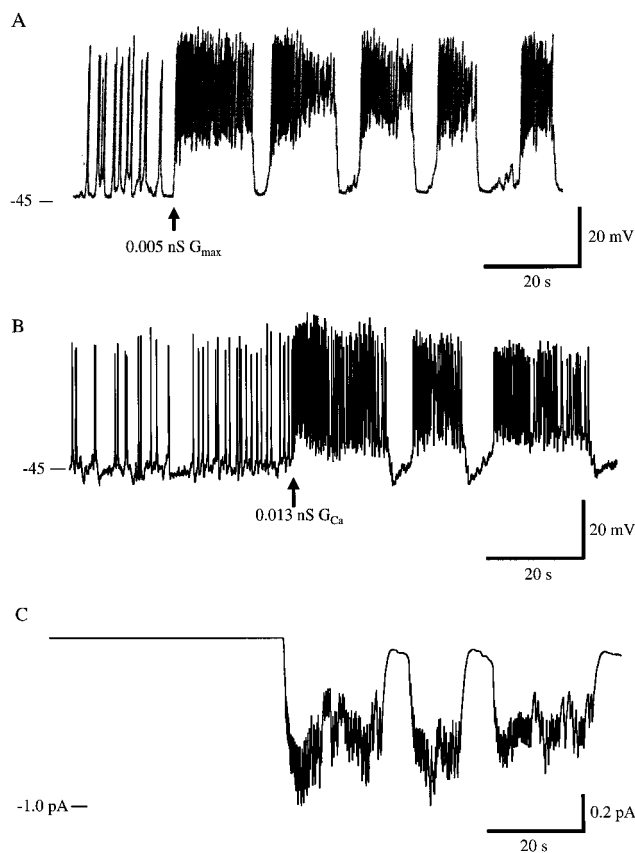
the exogenous current depolarized the membrane but did not elicit slower bursting.

As in the model, the exogenous current needed was very small, about 1 pA (Fig. 9 C). The results are robust in the sense that precise matching of the characteristics of the endogenous I_{s1} is not required (and, indeed, is not currently possible). However, it is far from the case that any depolarizing current will do. As expected from calculations with the model (not shown), if I_{Clamp} is too slow it is unable to induce medium bursting. This is shown in Fig. 10 A, where I_{Clamp} with $K = 0.02$ s^{-1} was applied with limited effect. The same cell was successfully converted to a slow rhythm by addition of the same amount of I_{Clamp} with $K = 2.0$ s^{-1}, the same rate constant used in the three examples in Fig. 9. If the exogenous current is too fast, it also fails to induce conversion; our best efforts using a dynamic clamp current with instantaneous activation have been able to lengthen burst duration of fast bursting cells only modestly (Fig. 12 of Kinard et al., 1999). Similarly, while nonspecific DC current was able to depolarize or drive cells into continuous
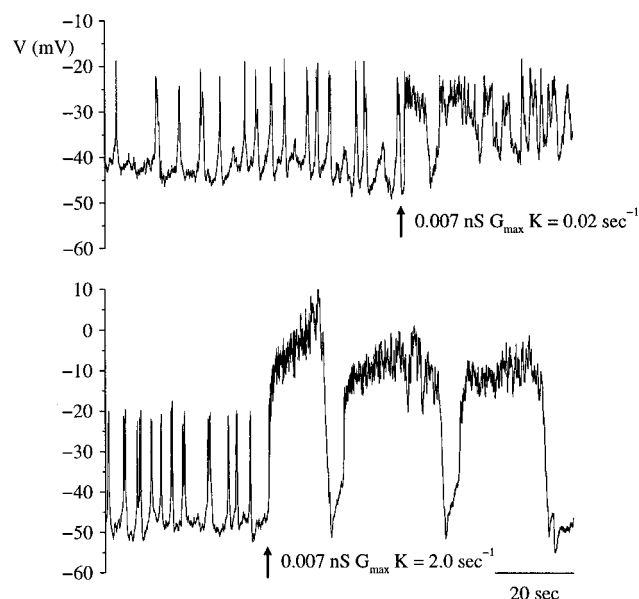
FIGURE 10 The effect of the activation rate constant, K, on conversion to slower firing. (*A*) The cell shows only a modest increase in period with $K = 0.02$ s^{-1}. (*B*) The same cell shows a much greater increase in period when $K = 2.0$ s^{-1}.

spiking, it was ineffective at converting fast bursting or spiking to medium bursting.

DISCUSSION

We have described a model of β-cell electrical activity with two slow conductances that can generate the full range of burst periods, from seconds to minutes, observed in pancreatic β-cells (Figs. 2–4). Of particular note is that the model can generate bursting oscillations with a period of 10 to 60 s, the range typically observed in islets. This phantom bursting is significant in light of the fact that no slow process with a medium-scale time constant has been identified in β-cells. Medium bursting in this model is controlled by a virtual pacemaker that emerges from the interaction of processes that are respectively much faster or slower than the medium time scale. There are several plausible candidates, discussed below, for variables that operate on these faster and slower scales.

The model presented here is highly idealized, employing the minimal elements needed to achieve our first modeling goal, explaining how fast, medium, and slow bursting might arise. Which of the three bursting modes is expressed depends on the maximal conductance, g_{s1}, of the faster of the two slow currents. When sufficient g_{s1} is present, it drives fast bursting, and as a result the slow s_2 current does not have enough time to oscillate. If g_{s1} is too small to terminate a burst even when its activation variable s_1 is maximal, s_2 comes into play. This is only one of a number of possible ways to switch from fast to medium or slow bursts with the

model; the key is to prevent the fast oscillations from pre-empting the slow ones. In the present version, reducing g_{s1} stretches the Z-shaped voltage nullcline (Fig. 7) so that it has multiple intersections with the s_1 nullcline, causing the trajectory to stall in the silent and active phases. Stretching or shifting the s_1 nullcline would have a similar effect, though with differences in detail. For concreteness, we chose s_1 and s_2 to be activation variables of hyperpolarizing K$^+$ currents, but versions of the model in which one or both of s_1 and s_2 are inactivation variables of depolarizing Ca^{2+} currents exhibit the same essential behavior.

Other ways of generating a wide range of oscillation periods have been considered previously. One way is to vary the time constant of the slow negative-feedback variable. For example, Atwater and Rinzel (1986) showed with the Chay-Keizer model that enhancing Ca^{2+} buffering increases the period by slowing the accumulation and clearance of cytosolic Ca^{2+}. This mechanism was not intended, however, to account for the full range of periods now known to exist. A second way is to stretch the range of values that the slow variable traverses in the course of a burst while keeping the rate of traversal the same. In recent models of Chay (1996, 1997), Ca_{er} is the slow variable, and its range is extended by reducing the flux of Ca^{2+} from the ER. It was suggested that β-cell cAMP levels in islets are greater than those in dispersed cells due to the paracrine secretion of glucagon by islet α-cells, which was expected to increase release rate and lead to faster bursting (Liu et al., 1998). The role of the ER in slow oscillations is assessed below. More generally, a serious comparison of models will require consideration of the full range of phenomena observed in β-cells and islets, including responses to glucose and to agonists that affect internal Ca^{2+} stores. The phantom model will have to be elaborated, at minimum incorporating equations for the cytosolic and ER Ca^{2+} concentrations and for ATP/ADP dynamics.

There are two leading candidate mechanisms for the slower variable, s_2, the concentration of Ca^{2+} in the endoplasmic reticulum (Ca_{er}) and activation of the K(ATP) channel conductance, and there are arguments both for and against each of these choices. There is some evidence that ER Ca^{2+} in β-cells varies on a several-minute time scale (Tengholm et al., 1998; Maechler et al., 1999), but it has not yet been demonstrated that ER Ca^{2+} oscillates in coincidence with bursting. There is also evidence for ER involvement in the minutes-long, biphasic transient seen when glucose is stepped from basal to stimulatory levels (Bertram et al., 1995; Mears et al., 1997). On the other hand, slow bursting persists in the presence of thapsigargin (Liu et al., 1995, 1998; Miura et al., 1997), an agent that irreversibly inhibits ER Ca^{2+} pumps and empties the ER.

K(ATP) channel conductance is known to be decreased by ATP and increased by ADP, and imaging data has shown that glycolytic intermediates and oxygen consumption oscillate accordingly, suggesting that the ATP/ADP ratio os-

cillates on a time scale appropriate for slow bursting (Longo et al., 1991; Nilsson et al., 1996). There is one report indicating variation in K(ATP) channel activity between active and silent phases during slow bursting (Larsson et al., 1996). In the models of Keizer and Magnus (1989, 1998), the ATP/ADP ratio declines as an indirect consequence of depolarization, which enhances Ca^{2+} flux into the mitochondria. This flux was hypothesized to decrease the rate of ATP production and, thus, ultimately to increase K(ATP) conductance.

In the simplified model here, s_2 represents the gating of a fictitious K^+ channel that opens very slowly in response to depolarization, but for the present purpose it does not make much difference whether a very slow K^+ conductance responds directly to membrane potential or indirectly through Ca^{2+}. We have verified that the actual Keizer-Magnus mechanism (Keizer and Magnus, 1989) can be incorporated in a phantom-type model with essentially identical results.

Detimary et al. (1998) have proposed an alternative mechanism for K(ATP) oscillations linked to membrane potential. They suggested that ATP is consumed by increased pumping of cytosolic Ca^{2+} out of the cell during the active phase of a burst, and recovers during the silent phase when Ca^{2+} declines. This mechanism can also be accommodated in a phantom-type model.

On the other hand, Smith et al. (1990) found no variation in K(ATP) conductance during slow bursting in single cells or small clusters. Miura et al. (1997) found that slow Ca^{2+} oscillations sometimes persist with K(ATP) blocked in islets, and Rosario et al. (1993) reported medium bursting with K(ATP) blocked. We note that if s_2 is interpreted as proportional to K(ATP) conductance, the model indicates that oscillations in K(ATP) conductance may be too small to be detected experimentally during medium bursting, whereas the oscillations would be more pronounced during slow bursting.

Candidates for s_1, the faster of the two slow variables in our model, include voltage-dependent inactivation of a depolarizing Ca^{2+} current and activation of a hyperpolarizing K(Ca) current. A component of Ca^{2+} current in β-cells with an inactivation time constant of a few seconds has been identified (Satin and Cook, 1988; Satin et al., 1994), and has been incorporated into several models (Chay and Cook, 1988; Keizer and Smolen, 1991). Medium bursting can be achieved in these models only by exaggerating the time constant of inactivation, but the measured values for the time constant are comparable to the range needed for τ_{s1} in the phantom model.

Recently, Göpel et al. (1999b) used patch clamp of single cells *in situ* in the periphery of islets to measure a K(Ca) current with time constants of 2.3 and 6.4 s for activation and deactivation, respectively, in response to simulated voltage bursts. Kozak et al. (1998) found what appears to be a similar current in an insulin-secreting cell line. The time

constants reported by Göpel et al. are broadly compatible with the phantom model, with K(Ca) playing the role of s_1.

Interestingly, Göpel et al. (1999b) report that their *in situ* current is much larger than a similar current in isolated cells, and suggest that this is why very slow bursting is seen in some isolated cells. This interpretation is consistent with the phantom model, with K(Ca) as the current gated by s_1. The phantom model further suggests that our isolated cells, which exhibit fast, rather than slow, oscillations (Rorsman and Trube, 1986; Falke et al., 1989; Kinard et al., 1999) may in contrast have a *surplus* of K(Ca) conductance. We do not yet know if this is the case or if fast cells differ from slow ones in some other way.

Our second modeling goal was to explain why medium bursting is not generally observed in isolated cells. Here we induced medium bursting in an artificial way by injecting exogenous current (Figs. 9 and 10). In an islet, cell-to-cell coupling current could play that role. As a preliminary demonstration of the feasibility of this hypothesis, Fig. 11 shows the effect of coupling a fast cell having high g_{s1} with a slow cell having low g_{s1}. When coupled, each cell behaves like a cell with an intermediate level of g_{s1} and bursts with a medium period. We conjecture that islets are composed of cells each of which is either fast or slow in isolation, depending on its balance of g_{s1} and g_{s2} or other parameters, but which synchronize to medium bursting *in situ*. Figure 11 illustrates a case in which the individual cells possess both fast and slow pacing processes (s_1 and s_2), but to different degrees. The end result would be similar if each cell had only s_1 or s_2; when coupled, it would behave as if it had both. Further experimental and theoretical work is needed in order to ascertain the actual distribution of cell properties in islets.
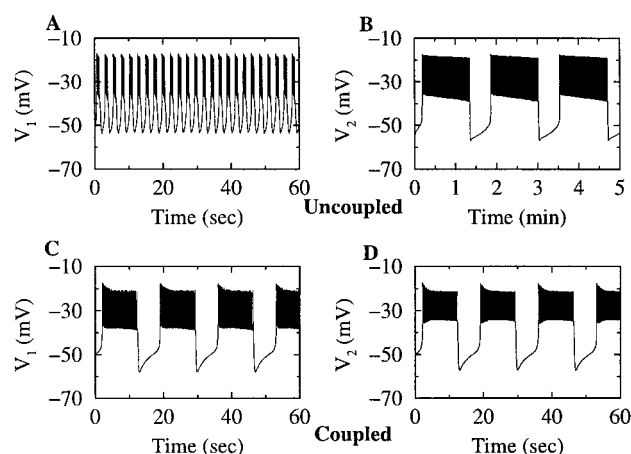

FIGURE 11 When a fast burster (g_{s1} = 20 pS, *A*) is coupled to a slow burster (g_{s1} = 3 pS, *B*) they synchronize in a medium bursting pattern (*C* and *D*). An islet composed of fast and slow cells could exhibit medium bursting even if the individual cells do not. Coupling added as in Smolen et al. (1993a); here, gap junction conductance is 130 pS. Note the different time scale in *B*.

Two other hypotheses addressing this question have been advanced previously, focusing on channel noise and cellular heterogeneity, respectively. According to the noise hypothesis, regular bursting is disrupted by channel fluctuations, resulting in either short bursts or continuous spiking activity (Atwater et al., 1983; Sherman et al., 1988; Chay and Kang, 1988). Though substantial noise is observed in single cells, this hypothesis is incompatible with the finding that there are slow oscillations in single cells and small cell clusters. A recent study of slow $[Ca^{2+}]_i$ oscillations in clusters of 1 to 50 islet cells found that the period of oscillation was several minutes in duration, nearly independent of the absolute number of cells, but was more regular in the larger clusters (Jonkers et al., 1999). Thus, although noise may play a more significant role in single cells and small clusters than in islets, it does not explain the gross differences in oscillations between single cells and islets.

According to the heterogeneity hypothesis, the variation of parameters among cells makes it unlikely that individual cells fall into the narrow parameter range needed for bursting (Smolen et al., 1993a), so that averaging of parameter values across the islet is needed for regular oscillations. The phantom model goes one step further in attempting to identify particular parameters that vary among cells and are capable of producing a wide range of burst periods.

In summary, we view this model not as the final answer to the problem of bursting in β-cells, but as a template for integrating a wide range of data and for posing questions. In addition to establishing a new theoretical framework, the model has already shown how to induce in isolated β-cells electrical activity like that of cells in islets. This defines a new experimental preparation that can facilitate the study of the ionic currents and other mechanisms involved in bursting under conditions in which bursting is actually seen and without interference from coupling artefacts.

REFERENCES

Atwater, I., C. M. Dawson, A. Scott, G. Eddlestone, and E. Rojas. 1980. The nature of the oscillatory behavior in electrical activity for pancreatic β-cell. *Horm. Metab. Res. Suppl.* 10:100–107.

Atwater, I., and J. Rinzel. 1986. The β-cell bursting pattern and intracellular $[Ca^{2+}]$. *In* Ionic channels in cells and model systems, R. Latorre, editor. Plenum Press, New York. 353–362.

Atwater, I., L. Rosario, and E. Rojas. 1983. Properties of calcium-activated potassium channels in the pancreatic β-cell. *Cell Calcium.* 4:451–461.

Barbosa, R. M., A. M. Silva, A. R. Tomé, J. A. Stamford, R. M. Santos, and L. M. Rosario. 1998. Control of pulsatile 5-HT/insulin secretion from single mouse pancreatic islets by intracellular calcium dynamics. *J. Physiol. (Lond.)* 510:135–143.

Bergsten, P. 1995. Slow and fast oscillations of cytosolic Ca^{2+} correspond to pulsatile insulin release. *Am. J. Physiol.* 268:E282–E287.

Bertram, R., A. Sherman, T. A. Kinard, and L. S. Satin. 2000. The phantom bursting model for pancreatic beta-cells. (abstr.) *Biophys. J.* 78:218A.

Bertram, R., P. Smolen, A. Sherman, D. Mears, I. Atwater, F. Martin, and B. Soria. 1995. A role for calcium release-activated current (CRAC) in cholinergic modulation of electrical activity in pancreatic β-cells. *Biophys. J.* 68:2323–2332.

Chay, T. R. 1996. Electrical bursting and luminal calcium oscillation in excitable cell models. *Biol. Cybern.* 75:419–431.

Chay, T. R. 1997. Effects of extracellular calcium on electrical bursting and intracellular and luminal calcium oscillations in insulin secreting pancreatic β-cells. *Biophys. J.* 73:1673–1688.

Chay, T. R., and D. L. Cook. 1988. Endogenous bursting patterns in excitable cells. *Math. Biosci.* 90:139–153.

Chay, T. R., and H. S. Kang. 1988. Role of single channel stochastic noise on bursting clusters of pancreatic β-cells. *Biophys. J.* 54:427–435.

Chay, T. R., and J. Keizer. 1983. Minimal model for membrane oscillations in the pancreatic β-cell. *Biophys. J.* 42:181–190.

Cook, D. L., and E. Perara. 1982. Islet electrical pacemaker response to alpha-adrenergic stimulation. *Diabetes.* 31:985–990.

Detimary, P., P. Gilon, and J.-C. Henquin. 1998. Interplay between cytoplasmic Ca^{2+} and the ATP/ADP ratio: a feedback control mechanism in mouse pancreatic islets. *Biochem. J.* 333:269–274.

Falke, L. C., K. D. Gillis, D. M. Pressel, and S. Misler. 1989. Perforated patch recording allows long-term monitoring of metabolite-induced electrical activity and voltage-dependent Ca^{2+} currents in pancreatic islet β cells. *FEBS Lett.* 251:167–172.

Gall, D., and I. Susa. 1999. Effects of Na/Ca exchange on plateau fraction and $[Ca]_i$ in models for bursting in pancreatic β-cells. *Biophys. J.* 77:45–53.

Gilon, P., and J.-C. Henquin. 1992. Influence of membrane potential changes on cytoplasmic Ca^{2+} concentration in an electrically excitable cell, the insulin-secreting pancreatic B-cell. *J. Biol. Chem.* 267:20713–20720.

Gilon, P., J. C. Jonas, and J. C. Henquin. 1994. Culture duration and conditions affect the oscillations of cytoplasmic calcium concentration induced by glucose in pancreatic islets. *Diabetologia.* 37:1007–1014.

Göpel, S., T. Kanno, S. Barg, J. Galvanovskis, and P. Rorsman. 1999a. Voltage-gated and resting membrane currents recorded from B-cells in intact mouse pancreatic islets. *J. Physiol.* 521:717–728.

Göpel, S. O., T. Kanno, S. Barg, L. Eliasson, J. Galvanovskis, E. Renström, and P. Rorsman. 1999b. Activation of Ca^{2+}-dependent K^+ channels contributes to rhythmic firing of action potentials in mouse pancreatic β cells. *J. Gen. Physiol.* 114:759–769.

Hamill, O. P., A. Marty, E. Neher, B. Sakmann, and F. J. Sigworth. 1981. Improved patch clamp techniques for high-resolution current recordings from cells and cell-free membrane patches. *Pflügers Arch.* 391:85–100.

Herrington, J., and R. J. Bookman. 1994. Pulse Control v4.3. Igor XOPs for Patch Clamp Data Acquisition. University of Miami Press, Miami, FL.

Hopkins, W., L. Satin, and D. L. Cook. 1991. Inactivation kinetics and pharmacology distinguish two calcium currents in mouse pancreatic β-cells. *J. Membr. Biol.* 119:229–239.

Jonkers, F., J.-C. Jonas, P. Gilon, and J.-C. Henquin. 1999. Influence of cell number on the characteristics and synchrony of Ca^{2+} oscillations in clusters of mouse pancreatic islet cells. *J. Physiol.* 520:839–849.

Keizer, J., and G. Magnus. 1989. ATP-sensitive potassium channel and bursting in the pancreatic β cell. *Biophys. J.* 56:229–242.

Keizer, J., and P. Smolen. 1991. Bursting electrical activity in pancreatic β cells caused by Ca^{2+}- and voltage-inactivated Ca^{2+} channels. *Proc. Natl. Acad. Sci. USA.* 88:3897–3901.

Kinard, T. A., G. de Vries, A. Sherman, and L. S. Satin. 1999. Modulation of the bursting properties of single mouse pancreatic β-cells by artificial conductances. *Biophys. J.* 76:1423–1435.

Kinard, T. A., and L. S. Satin. 1996. Temperature modulates the Ca^{2+} current of HIT-T15 and mouse pancreatic β-cells. *Cell Calcium.* 20: 475–482.

Kozak, J. A., S. Misler, and D. E. Logothetis. 1998. Characterization of a Ca^{2+}-activated K^+ current in insulin-secreting murine βTC-3 cells. *J. Physiol. (Lond.)* 509:355–370.

Larsson, O., H. Kindmark, R. Bränström, B. Fredholm, and P.-O. Berggren. 1996. Oscillations in K_{ATP} channel activity promote oscillations in cytoplasmic free Ca^{2+} concentration in the pancreatic β-cell. *Proc. Natl. Acad. Sci. USA.* 93:5161–5165.

Leech, C. A., G. G. Holz IV, and J. F. Habener. 1994. Voltage-independent calcium channels mediate slow oscillations of cytosolic calcium that are glucose dependent in pancreatic β-cells. *Endocrinology.* 135:365–372.

Liu, Y.-J., E. Grapengiesser, E. Gylfe, and B. Hellman. 1994. Glucose-induced oscillations of Ba^{2+} in pancreatic β-cells occur without involvement of intracellular mobilization. *Arch. Biochem. Biophys.* 315: 387–392.

Liu, Y.-J., E. Grapengiesser, E. Gylfe, and B. Hellman. 1995. Glucose induces oscillations of cytoplasmic Ca^{2+}, Sr^{2+} and Ba^{2+} in pancreatic β-cells without participation of the thapsigargin-sensitive store. *Cell Calcium.* 18:165–173.

Liu, Y.-J., A. Tengholm, E. Grapengiesser, B. Hellman, and E. Gylfe. 1998. Origin of slow and fast oscillations of Ca^{2+} in mouse pancreatic islets. *J. Physiol. (Lond.)* 508:471–481.

Longo, E. A., K. Tornheim, J. T. Deeney, B. A. Varnum, D. Tillotson, M. Prentki, and B. E. Corkey. 1991. Oscillations in cytosolic free Ca^{2+}, oxygen consumption, and insulin secretion in glucose-stimulated rat pancreatic islets. *J. Biol. Chem.* 266:9314–9319.

Ma, M., and J. Koester. 1996. The role of K^+ currents in frequency-dependent spike broadening in Aplysia R20 neurons: a dynamic-clamp analysis. *J. Neurosci.* 16:4089–4101.

Maechler, P., E. D. Kennedy, E. Sebö, A. Valeva, T. Pozzan, and C. B. Wollheim. 1999. Secretagogues modulate the calcium concentration in the endoplasmic reticulum of insulin-secreting cells. *J. Biol. Chem.* 274:12583–12592.

Magnus, G., and J. Keizer. 1998. Model of β-cell mitochondrial calcium handling and electrical activity. I Cytoplasmic variables. *Am. J. Physiol.* 274:C1158–C1173.

Martin, F., J. V. Sanchez-Andres, and B. Soria. 1995. Slow $[Ca^{2+}]_i$ oscillations induced by ketoisocaproate in single mouse pancreatic islets. *Diabetes.* 44:300–305.

Martin, F., and B. Soria. 1995. Amino acid-induced $[Ca^{2+}]_i$ oscillations in single mouse pancreatic islets. *J. Physiol. (Lond.)* 486:361–371.

Mears, D., N. F. Sheppard, Jr., I. Atwater, E. Rojas, R. Bertram, and A. Sherman. 1997. Evidence that calcium release-activated current mediates transient glucose-induced electrical activity in the pancreatic β-cell. *J. Membr. Biol.* 155:47–59.

Miura, Y., J.-C. Henquin, and P. Gilon. 1997. Emptying of intracellular Ca^{2+} stores stimulates Ca^{2+} entry in mouse pancreatic β-cells by both direct and indirect mechanisms. *J. Physiol. (Lond.)* 503:387–398.

Nilsson, T., V. Schultz, P.-O. Berggren, B. E. Corkey, and K. Tornheim. 1996. Temporal patterns of changes in ATP/ADP ratio, glucose 6-phosphate and cytoplasmic free Ca^{2+} in glucose-stimulated pancreatic β-cells. *Biochem. J.* 314:91–94.

Rae, J., K. Cooper, P. Gates, and M. Watsky. 1991. Low access resistance perforated patch recordings using amphotericin B. *J. Neurosci. Methods.* 37:15–26.

Rinzel, J., and B. Ermentrout. 1998. Analysis of neural excitability and oscillations. *In* Methods in Neuronal Modeling. C. Koch and I. Segev, editors. The MIT Press, Cambridge, MA. 251–291.

Roe, M. W., B. Spencer, M. E. Lancaster, R. J. Mertz, J. F. Worley, III, and I. D. Dukes. 1995. Absence of effect of culture duration on glucose-activated alterations in intracellular calcium concentration in mouse pancreatic islets. *Diabetologia.* 38:876–879.

Roe, M. W., J. F. Worley, III, F. Qian, N. Tamarina, A. A. Mittal, F. Dralyuk, N. T. Blair, R. J. Mertz, L. H. Philipson, and I. D. Dukes. 1998. Characterization of a Ca^{2+} release-activated nonselective cation current regulating membrane potential and $[Ca^{2+}]_i$ oscillations in transgenically derived β-cells. *J. Biol. Chem.* 273:10402–10410.

Rorsman, P., and G. Trube. 1986. Calcium and delayed potassium currents in mouse pancreatic β-cells under voltage clamp conditions. *J. Physiol. (Lond.)* 374:531–550.

Rosario, L. M., R. M. Barbosa, C. M. Antunes, A. M. Silva, A. J. Abrunhosa, and R. M. Santos. 1993. Bursting electrical activity in pancreatic β-cells: evidence that the channel underlying the burst is sensitive to Ca^{2+} influx through L-type Ca^{2+} channels. *Pflügers Arch.* 424:439–447.

Sánchez-Andrés, J., A. Gomis, and M. Valdeolmillos. 1995. The electrical activity of mouse pancreatic β-cells recorded in vivo shows glucose-dependent oscillations. *J. Physiol. (Lond.)* 486:223–228.

Satin, L. S., and D. L. Cook. 1988. Evidence for two calcium currents in insulin-secreting cells. *Pflügers Arch.* 411:401–409.

Satin, L. S., S. J. Tavalin, and P. Smolen. 1994. Calcium channel inactivation in HIT cells studied with an imposed burst waveform. *Biophys. J.* 66:141–148.

Sharp, A. A., M. B. O'Neil, L. F. Abbott, and E. Marder. 1993. Dynamic clamp: computer generated conductances in real neurons. *J. Neurophysiol.* 69:992–995.

Sherman, A., J. Rinzel, and J. Keizer. 1988. Emergence of organized bursting in clusters of pancreatic β-cells by channel sharing. *Biophys. J.* 54:411–425.

Smith, P. A., F. M. Ashcroft, and P. Rorsman. 1990. Simultaneous recordings of glucose dependent electrical activity and ATP-regulated K^+-currents in isolated mouse pancreatic β-cells. *FEBS Lett.* 261:187–190.

Smolen, P., and J. Keizer. 1992. Slow voltage inactivation of Ca^{2+} currents and bursting mechanisms for the mouse pancreatic β-cell. *J. Membr. Biol.* 127:9–19.

Smolen, P., J. Rinzel, and A. Sherman. 1993a. Why pancreatic islets burst but single β-cells do not: the heterogeneity hypothesis. *Biophys. J.* 64:1668–1679.

Smolen, P., D. Terman, and J. Rinzel. 1993b. Properties of a bursting model with two slow inhibitory variables. *SIAM J. Appl. Math.* 53: 861–892.

Tengholm, A., C. Hagman, E. Gylfe, and B. Hellman. 1998. In situ characterization of nonmitochondrial Ca^{2+} stores in individual pancreatic β-cells. *Diabetes.* 47:1224–1230.

Turrigiano, G. G., E. Marder, and L. F. Abbott. 1996. Cellular short-term memory from a slow potassium conductance. *J. Neurophysiol.* 75: 963–966.